

Original Research Paper

## Optimizing a low-temperature combustion engine run with various compression ratios using the modified social group technique

Seyed Mohammad Safieddin Ardebili<sup>1\*</sup>, Ibhram Veza<sup>2</sup>, Aslan Deniz Karaoglan<sup>3</sup>, Erol Ileri<sup>4</sup>, Mostafa Kiani Deh Kiani<sup>5</sup>, Masoud Rabeti<sup>6</sup>

<sup>1</sup> Department of Biosystems Engineering, Shahid Chamran University of Ahvaz, Ahvaz, Iran

<sup>2</sup> Department of Mechanical Engineering, Faculty of Engineering, Universitas Bung Karno, Jakarta Pusat, Indonesia

<sup>3</sup> Balikesir University, Department of Industrial Engineering, 10145 Balikesir, Turkey

<sup>4</sup> National Defense University, Army NCO Vocational HE School, Department of Automotive Sciences, 10110 Balikesir, Turkey

<sup>5</sup> Department of Biosystems Engineering, Shahid Chamran University of Ahvaz, Ahvaz, Iran

<sup>6</sup> Department of Mechanical Engineering, Faculty of Engineering, Sousangerd Branch, Islamic Azad University, Sousangerd, Iran

Biosystems Engineering and Renewable Energies 2025, 1 (1): 11-20

### KEYWORDS

Social group optimization  
Regression modeling optimization  
HCCI optimization  
HCCI performance

### \* Corresponding author

m.safieddin@scu.ac.ir

### Article history

Received: 2024-11-3

Revised: 2024-11-13

Accepted: 2024-12-17

### ABSTRACT

This low-temperature combustion study modified a single-cylinder gasoline engine into an HCCI engine. For the HCCI experiments, four different compression ratios were used. The intake air temperatures varied between 313 and 373 K, while the engine speed changed from 800 to 1800 rpm. Three fuel blends were used. The RON60 indicates 60% iso-octane and 40% n-heptane. A modified social group optimization algorithm was used for HCCI optimization purposes. Regression modeling was first employed to calculate the mathematical relations between the factors (i.e., compression ratio, research octane number, intake air temperature, engine speed, and lambda) and the responses (effective torque, IMEP, indicated thermal efficiency, specific fuel consumption, COV IMEP, and HC). For the HCCI performance tests, the regression models fit the given observations well with a low prediction error. The calculated  $R^2$  obtained from this study shows that the compression ratio ( $X_1$ ), RON ( $X_2$ ), intake air temperature ( $X_3$ ), engine speed ( $X_4$ ), and lambda ( $X_5$ ) are sufficient to model the responses (effective torque, IMEP, indicated thermal efficiency, specific fuel consumption, COV IMEP, and HC). Then, the MSGO is run via these mathematical models to determine the parameters with optimal optimization values. In the verification phase, 13 additional experimental runs that were not used in the mathematical modeling phase were used. It was found that the regression models fit the observed values well with a low PE (%). The algorithm suggested the best value for studied parameters as  $X_1 = 11.47$ ,  $X_2 = 60$ ,  $X_3 = 313$  K,  $X_4 = 800$  rpm, and  $X_5 = 1.45$ . The verification shows satisfying results with a high accuracy. The optimized factor levels indicate that the effective torque, IMEP, and indicated thermal efficiency were maximized while the other responses were minimized. Therefore, the findings signify the potential of the algorithm for HCCI optimization.

## 1. Introduction

The increasingly stringent emissions regulation has enforced the development of engine technology. The goal is to push current vehicles to produce ultra-low emissions with acceptable performance. Recent developments in conventional internal combustion engines (ICE) have made it possible to improve their emissions and fuel consumption. Using a three-way catalytic converter can significantly reduce the CO, HC, and NO<sub>x</sub> emissions of gasoline engines. However, the operation of lean air-fuel ratio (AFR) is impossible at part load as the conversion efficiencies can only be maintained close to stoichiometry. As a result, a significant increase in fuel consumption of a gasoline engine cannot be avoided. On the other hand, the lean AFR can be achieved using stratified charge gasoline direct injection (GDI). Both technologies enable the fuel flow rate to be changed regardless of the airflow, thus varying the load independently of the airflow. However, using a lean mixture prevents the effectiveness of NO<sub>x</sub> after treatments.

Homogeneous charge compression ignition (HCCI) technology emerges as a promising concept (Kocakulak et al., 2023). HCCI engines can satisfy stringent emissions regulations with

acceptable engine performance without the use of expensive, complex, and inefficient after-treatment systems (Abdelmalek et al., 2021; Kocakulak et al., 2022). Its combustion differs from that of the conventional combustion of spark ignition (SI) or compression ignition (CI). Unlike the flame propagation of SI engine or diffusion combustion of CI engine, the combustion in HCCI engine occurs by a combination of a diluted and premixed fuel and air mixture (Parsa and Neshat, 2022). Such a homogeneous mixture ignites simultaneously at multiple locations inside the combustion chamber. Therefore, the hot flame zone or high combustion temperature region that will produce NO<sub>x</sub> emissions can be avoided. Moreover, the premixed mixture helps prevent the rich fuel mixture, thus reducing soot emissions substantially. Due to the simultaneous reduction of both NO<sub>x</sub> and soot, HCCI combustion emerges as a promising technology compared to conventional SI and CI engine that suffers from the trade-off of NO<sub>x</sub>-soot emissions. The lean mixture also allows the HCCI to be run unthrottled, thus increasing the engine efficiency and improving the fuel economy compared to the SI engine. Note that the HCCI engine is not yet available in the market. Thus, a

modification is normally performed using traditional gasoline or diesel engines for research purposes.

Artificial intelligence-based methods such as artificial neural networks (ANN) and adaptive network-based fuzzy inference systems (ANFIS) have attracted recent attention (Deh Kiani et al., 2010; Leo et al., 2020). Optimization techniques, in particular, have an important effect on solving several engineering issues. Deterministic techniques are computationally expensive and difficult to reach a useful solution for real-life problems, which are often indicated by their complex nonlinearity and multimodal characteristics (AlShabi et al., 2021). Meta-heuristic algorithms are therefore considered more efficient for solving practical problems since they are stochastic and derivative-free (Rao and Keesari, 2020; Roushangar and Shahnazi, 2019; Tejani et al., 2018).

Inspired by nature to overcome complicated real-world problems, meta-heuristic algorithms have attracted a lot of attention. They depend on simulating nature and are commonly used to solve optimization problems (especially global optimization) (Yazdani and Jolai, 2015). There are several types of meta-heuristic algorithms including particle swarm optimization (PSO), genetic algorithm (GA), social group optimization (SGO), modified social group optimization (MSGO), ant colony optimization (ACO), and harmony search (HS) which are frequently used for modeling of different engineering issues (Bhadoria and Marwaha, 2020). A systematic review containing the meta-heuristic techniques has been published and critically discussed by Naik et al. (2020).

There are two significant aspects that are in contrast to each other in the heuristic optimization methods: (i) exploration and (ii) exploitation. Exploration means seeking the entire space and having different answers for each iteration (global search), while exploitation refers to the quality of the solution for every iteration (local search). Too much reliance on exploitation may lead to being stuck in local optimum points, yet too much concentrating on exploration may result in the low worth of the last best solution (Eiben and Schippers, 1998). Therefore, an algorithm must be capable of balancing these two factors.

Among the human-based algorithms illustrated, the SGO invented by Satapathy and Naik (2016) has attracted more attention recently. SGO is inspired by the social manner of an individual in a group to solve complicated problems. SGO has been applied effectively for solving optimization problems. Progress of the SGO algorithm is composed of two phases: (i) improving and (ii) acquiring. During the improvement phase, each individual expands his or her knowledge by interacting with the best person in the group (best solution). To acquire knowledge, individuals interact with randomly selected individuals and the best person at the same time during the acquiring phase. SGO has been improved and is now known as modified SGO (MSGO). The MSGO improves the acquiring phase of SGO and introduces a self-awareness probability factor. In this way, an individual's learning capability from the best-learned person in the societal setup is enhanced (Naik et al., 2020; Satapathy and Naik, 2016).

Although the SGO algorithm gave an improvement in the exploration and exploration search ability compared to other several algorithms, however, this technique currently is not capable of finding the optimal point for some functions of fixed-dimensional multimodal (Mirjalili and Lewis, 2016). Therefore, it is necessary to balance the exploration and exploration search ability using the MSGO. Its performance has been investigated by mimicking benchmark functions employed by previous studies (Heidari et al., 2019; Mirjalili, 2016; Mirjalili et al., 2014; Moghdani and Salimifard, 2018; Nematollahi et al., 2017; Nematollahi et al., 2020; Shareef et al., 2015; Zhao et al., 2019).

Although several studies have indicated promising findings applying the MSGO algorithm, there is no available work evaluating the usefulness of the MSGO for internal combustion engines (ICE) application, particularly for low-temperature combustion HCCI engines. Therefore, this investigation is devoted

to studying the MSGO method as a novel technique to optimize LTC combustion. Despite the promise of electric vehicles, ICEs are still being actively researched owing to their application for other purposes, such as marine engines. HCCI engine, for instance, has the potential to be the next ICE technology as it can be run using different types of fuels and can be utilized to extend the range of electric vehicles.

In the present study, the multi-objective optimization based on the MSGO algorithm was utilized to determine the optimal values of engine parameters (i.e., compression ratio, research octane number (RON), intake air temperature, engine speed, and lambda) and the engine-out factors (i.e., effective torque, IMEP, indicated thermal efficiency, specific fuel consumption, COV IMEP, and HC. The coefficient of variation in indicated mean effective pressure (COV IMEP) was used to assess combustion stability as it represents the cyclic variability.

## 2. Materials and Methods

### 2.1. Experimental setup and test fuels

In this study, the single-cylinder gasoline engine was modified into an HCCI engine. The schematic diagram of the engine setup with its detailed characteristics is given in Table 1. In the experiments, four different compression ratios were used (CR9, CR10, CR11, and CR12). The intake air temperatures varied between 313 and 373 K, while the engine speed changed from 800 to 1800 rpm. Three fuel blends, i.e., RON20, RON40, and RON60, were used. The RON60 indicates 60% iso-octane and 40% n-heptane. The physicochemical properties of iso-octane and n-heptane fuels are presented in Table 2. The detailed experimental setup has been previously explained (Calam et al., 2019).

### 2.2. Optimization using the MSGO

In SGO and MSGO, each individual (person) of the group shows a potential solution, and the number of design variables in the problem is represented by the human traits, which represent a person's dimension. The pseudocode for the improving phase is given in Eqs. (1) and (2). In this equation,  $P_i$  is the persons of the social group that is composed of  $N$  persons where  $i = \{1, 2, 3, \dots, N\}$ . In addition, each person also has  $D$  traits ( $P_i = P_{i1}, P_{i2}, \dots, P_{iD}$ ). By doing so,  $gbest$  will be able to help others in the group improve their knowledge. The aim is formulated as a minimization problem in Eq. (1) (Naik, 2021; Naik et al., 2020; Satapathy and Naik, 2016)

**Table 1.** The specification of the engine.

| Test Engine                | Ricardo Hydra           |
|----------------------------|-------------------------|
| Cylinder number            | 1                       |
| Bore x stroke (mm)         | 80.26 x 88.90           |
| Compression ratio          | 5:1 - 13:1              |
| Maximum power output (kW)  | 15                      |
| Maximum engine speed (rpm) | 5400                    |
| Fuel injection system      | Port injection          |
| Valve lift (mm)            | Intake 5.5, exhaust 3.5 |

**Table 2.** Physicochemical properties of n-heptane/iso-octane.

| Properties                            | iso-octane                     | n-heptane                      |
|---------------------------------------|--------------------------------|--------------------------------|
| RON                                   | 0                              | 100                            |
| Chemical formula                      | C <sub>7</sub> H <sub>16</sub> | C <sub>8</sub> H <sub>18</sub> |
| Molar mass (g/mol)                    | 100.21                         | 114.23                         |
| Density (kg/cm <sup>3</sup> at 20 °C) | 0.68                           | 0.69                           |
| Boiling point (°C)                    | 97-98                          | 99                             |
| Lower heat value (kJ/kg)              | 44566                          | 44310                          |

$$[\min \text{value}, \text{index}] = \min\{f(P_i), i = 1, 2, \dots, N\} \quad (1)$$

$$gbest = P(\text{index}, :) \quad (2)$$

where  $P_i$  values are the updated values at the end of the enhancing stage. In this paper, some of the codes used from the following references and the assumption in this code were considered as  $\text{rand}_1 \sim U(0,1)$  and  $\text{rand}_2 \sim U(0,1)$  are used to affect the algorithm's stochastic nature (Naik et al., 2020; Satapathy and Naik, 2016).

The MSGO algorithm was developed by modifying the acquiring phase of the SGO algorithm. The improving phase is the same as in SGO. In this phase, each social group member continues to interact with the best person ( $best_p$ ). Also, each person interacts with the other group members to acquire knowledge. If the other person has more knowledge, the person acquires new knowledge during this phase.

Also, the SAP was selected as a capacity to acquire knowledge from another person. The acquiring phase of MSGO was calculated as a minimization problem which is depicted in Eq. (3) (Naik, 2021; Naik et al., 2020; Satapathy and Naik, 2016).

$$[value, index - num] = \min\{f(P_i), i = 1, 2, \dots, N\}$$

and

$$gbest_p = P(index - num, :) \tag{3}$$

In the modified code used in this paper, it is proposed to select the SAP between 0.6 and 0.9. According to the literature, MSGO shows the best performance for SAP=0.7 and  $c=0.2$  (Naik, 2021; Naik et al., 2020; Satapathy and Naik, 2016).

### 3. Results and Discussion

This investigation was performed in three steps, including performing the experimental runs, fitting mathematical models, and finally, the optimization by using the MSGO method. Table 3 presents the minimum and maximum levels of the factors utilized in the experiments.

An experimental design with 48 test runs was conducted for the different combinations of these factors. Table 4 represents the coded and uncoded factor levels together. In the mathematical modeling phase (second stage), regression models of the responses ( $Y_1$ : effective torque (Nm),  $Y_2$ : IMEP (Bar),  $Y_3$ : indicated thermal efficiency,  $Y_4$ : specific fuel consumption (g/kWh),  $Y_5$ : COV IMEP (%), and  $Y_6$ : HC (ppm)) were generated for both coded/uncoded factors. Using coded factor levels is based on the requirement to use mathematical models for the coded factor levels in the optimization stage. However, in order to show the true mathematical relationship to readers, the original models (the models with uncoded factor levels) were also computed. Accordingly, in Table 4, coded factor levels are presented alongside uncoded factor levels. The coding is carried out using Eq. (4).

$$X_{coded} = \frac{(X_{uncoded} - ((X_{max} + X_{min})/2))}{((X_{max} - X_{min})/2)} \tag{4}$$

**Table 3.** Minimum and maximum levels of the factors utilized in the experiments

| Factors                | Symbols | Unit | Levels |      |
|------------------------|---------|------|--------|------|
|                        |         |      | min    | max  |
| Compression ratio      | $X_1$   | -    | 9      | 12   |
| RON                    | $X_2$   | -    | 20     | 60   |
| Intake air temperature | $X_3$   | K    | 313    | 373  |
| Engine speed           | $X_4$   | rpm  | 800    | 1800 |
| Lambda                 | $X_5$   | -    | 1.09   | 2.96 |

**Table 4.** The experimental results

| Run (i) | Factors (Uncoded) |          |          | $X_{i4}$ | $X_{i5}$ | Factors (Coded) |          |          | $X_{i4}$ | $X_{i5}$ | Responses |          |          |          |          |          |
|---------|-------------------|----------|----------|----------|----------|-----------------|----------|----------|----------|----------|-----------|----------|----------|----------|----------|----------|
|         | $X_{i1}$          | $X_{i2}$ | $X_{i3}$ |          |          | $X_{i1}$        | $X_{i2}$ | $X_{i3}$ |          |          | $Y_{i1}$  | $Y_{i2}$ | $Y_{i3}$ | $Y_{i4}$ | $Y_{i5}$ | $Y_{i6}$ |
| 1       | 9                 | 20       | 353      | 1800     | 1.71     | -1.00           | -1.00    | 0.33     | 1.00     | -0.34    | 6.78      | 4.6021   | 0.2426   | 322.7165 | 4.2591   | 392      |
| 2       | 9                 | 20       | 373      | 800      | 1.6      | -1.00           | -1.00    | 1.00     | -1.00    | -0.45    | 9.45      | 4.7936   | 0.2921   | 283.5195 | 3.2179   | 687.8    |
| 3       | 9                 | 20       | 373      | 1200     | 1.68     | -1.00           | -1.00    | 1.00     | -0.20    | -0.37    | 8.42      | 4.6372   | 0.2745   | 288.2594 | 3.7815   | 585.8    |
| 4       | 9                 | 20       | 373      | 1200     | 1.99     | -1.00           | -1.00    | 1.00     | -0.20    | -0.04    | 7.86      | 4.3537   | 0.2926   | 282.0633 | 3.2681   | 567.6    |
| 5       | 9                 | 40       | 373      | 800      | 1.63     | -1.00           | 0.00     | 1.00     | -1.00    | -0.42    | 8.80      | 5.0232   | 0.2731   | 275.1285 | 2.7790   | 543      |
| 6       | 9                 | 40       | 373      | 1200     | 1.5      | -1.00           | 0.00     | 1.00     | -0.20    | -0.56    | 8.34      | 5.6865   | 0.2609   | 284.6162 | 4.1903   | 397      |
| 7       | 10                | 20       | 313      | 1600     | 1.97     | -0.33           | -1.00    | -1.00    | 0.60     | -0.06    | 5.30      | 5.1018   | 0.2872   | 271.9470 | 3.4947   | 405      |
| 8       | 10                | 40       | 313      | 800      | 1.09     | -0.33           | 0.00     | -1.00    | -1.00    | -1.00    | 12.45     | 9.0492   | 0.3186   | 255.7469 | 3.2958   | 488      |
| 9       | 10                | 40       | 313      | 800      | 1.38     | -0.33           | 0.00     | -1.00    | -1.00    | -0.69    | 10.92     | 7.2743   | 0.3361   | 251.9483 | 2.2293   | 461      |
| 10      | 10                | 40       | 333      | 1200     | 1.81     | -0.33           | 0.00     | -0.33    | -0.20    | -0.23    | 8.75      | 5.8968   | 0.3042   | 269.0526 | 2.7163   | 360.8    |
| 11      | 10                | 40       | 353      | 1000     | 2.31     | -0.33           | 0.00     | 0.33     | -0.60    | 0.30     | 6.92      | 4.8480   | 0.3139   | 266.0762 | 2.3521   | 389      |
| 12      | 10                | 40       | 353      | 1200     | 1.92     | -0.33           | 0.00     | 0.33     | -0.20    | -0.11    | 8.05      | 5.4741   | 0.3027   | 273.9515 | 2.6530   | 366.2    |
| 13      | 10                | 40       | 353      | 1600     | 1.68     | -0.33           | 0.00     | 0.33     | 0.60     | -0.37    | 7.17      | 6.0306   | 0.2544   | 305.7614 | 3.2636   | 263.6    |
| 14      | 10                | 60       | 353      | 800      | 1.6      | -0.33           | 1.00     | 0.33     | -1.00    | -0.45    | 8.69      | 6.8475   | 0.2933   | 271.9648 | 2.8531   | 296.8    |
| 15      | 10                | 60       | 353      | 1000     | 1.65     | -0.33           | 1.00     | 0.33     | -0.60    | -0.40    | 7.69      | 6.3437   | 0.2806   | 282.9162 | 2.9758   | 242.8    |
| 16      | 11                | 40       | 353      | 800      | 2.56     | 0.33            | 0.00     | 0.33     | -1.00    | 0.57     | 7.66      | 4.3431   | 0.3050   | 266.4178 | 2.2151   | 373      |
| 17      | 11                | 60       | 373      | 800      | 1.58     | 0.33            | 1.00     | 1.00     | -1.00    | -0.48    | 10.72     | 5.6842   | 0.3041   | 269.8903 | 3.1181   | 400      |
| 18      | 11                | 60       | 373      | 800      | 1.68     | 0.33            | 1.00     | 1.00     | -1.00    | -0.37    | 10.23     | 5.5270   | 0.3110   | 264.1549 | 2.8594   | 392      |
| 19      | 12                | 20       | 313      | 800      | 2.89     | 1.00            | -1.00    | -1.00    | -1.00    | 0.93     | 6.55      | 4.4590   | 0.2974   | 253.7486 | 3.1165   | 429.4    |
| 20      | 12                | 20       | 313      | 1000     | 1.65     | 1.00            | -1.00    | -1.00    | -0.60    | -0.40    | 10.10     | 5.0902   | 0.3468   | 249.1402 | 4.4875   | 372.4    |
| 21      | 12                | 20       | 313      | 1000     | 1.76     | 1.00            | -1.00    | -1.00    | -0.60    | -0.28    | 8.84      | 5.0346   | 0.3534   | 245.4160 | 4.3285   | 342      |
| 22      | 12                | 20       | 313      | 1200     | 1.71     | 1.00            | -1.00    | -1.00    | -0.20    | -0.34    | 9.33      | 5.1852   | 0.3206   | 259.4196 | 4.4580   | 378.6    |
| 23      | 12                | 20       | 313      | 1200     | 1.9      | 1.00            | -1.00    | -1.00    | -0.20    | -0.13    | 7.45      | 4.9164   | 0.3370   | 255.5125 | 4.2378   | 381.4    |
| 24      | 12                | 20       | 313      | 1200     | 2.18     | 1.00            | -1.00    | -1.00    | -0.20    | 0.17     | 6.85      | 4.8853   | 0.3111   | 260.2514 | 4.0944   | 393.6    |
| 25      | 12                | 20       | 313      | 1400     | 1.82     | 1.00            | -1.00    | -1.00    | 0.20     | -0.22    | 7.20      | 5.1706   | 0.3182   | 264.5130 | 4.5103   | 373.6    |
| 26      | 12                | 20       | 313      | 1400     | 2.18     | 1.00            | -1.00    | -1.00    | 0.20     | 0.17     | 7.05      | 4.7074   | 0.3004   | 269.9124 | 4.3153   | 376.6    |
| 27      | 12                | 20       | 313      | 1600     | 1.94     | 1.00            | -1.00    | -1.00    | 0.60     | -0.09    | 6.65      | 5.0727   | 0.2967   | 275.5102 | 4.4862   | 365      |
| 28      | 12                | 20       | 373      | 800      | 2.96     | 1.00            | -1.00    | 1.00     | -1.00    | 1.00     | 6.65      | 3.5905   | 0.2522   | 279.6359 | 3.8023   | 343      |
| 29      | 12                | 40       | 313      | 800      | 1.67     | 1.00            | 0.00     | -1.00    | -1.00    | -0.38    | 15.45     | 6.5019   | 0.3688   | 227.8163 | 3.0670   | 518.4    |
| 30      | 12                | 40       | 313      | 1000     | 1.71     | 1.00            | 0.00     | -1.00    | -0.60    | -0.34    | 14.59     | 6.2734   | 0.3418   | 236.6185 | 3.1385   | 496      |
| 31      | 12                | 40       | 313      | 1200     | 1.77     | 1.00            | 0.00     | -1.00    | -0.20    | -0.27    | 15.26     | 5.9747   | 0.3468   | 242.6032 | 3.5470   | 446.6    |
| 32      | 12                | 40       | 333      | 800      | 1.69     | 1.00            | 0.00     | -0.33    | -1.00    | -0.36    | 15.80     | 5.2893   | 0.3457   | 236.8163 | 3.1481   | 421.6    |
| 33      | 12                | 40       | 333      | 1000     | 1.76     | 1.00            | 0.00     | -0.33    | -0.60    | -0.28    | 15.70     | 5.2188   | 0.3507   | 237.6496 | 3.3059   | 408.2    |
| 34      | 12                | 40       | 353      | 800      | 1.71     | 1.00            | 0.00     | 0.33     | -1.00    | -0.34    | 15.34     | 4.9084   | 0.3403   | 241.8164 | 3.3942   | 359.8    |
| 35      | 12                | 40       | 353      | 1200     | 2.43     | 1.00            | 0.00     | 0.33     | -0.20    | 0.43     | 9.57      | 4.2494   | 0.3141   | 255.4630 | 3.2350   | 372      |
| 36      | 12                | 40       | 373      | 800      | 1.74     | 1.00            | 0.00     | 1.00     | -1.00    | -0.30    | 12.58     | 4.4634   | 0.3279   | 247.1163 | 3.8470   | 395      |
| 37      | 12                | 40       | 373      | 1200     | 1.94     | 1.00            | 0.00     | 1.00     | -0.20    | -0.09    | 10.72     | 4.4578   | 0.3303   | 240.7826 | 4.1356   | 346.4    |

**Table 4.** Continued.

| Run (i) | Factors (Uncoded) |          |          |          |          | Factors (Coded) |          |          |          |          | Responses |          |          |          |          |          |
|---------|-------------------|----------|----------|----------|----------|-----------------|----------|----------|----------|----------|-----------|----------|----------|----------|----------|----------|
|         | $X_{i1}$          | $X_{i2}$ | $X_{i3}$ | $X_{i4}$ | $X_{i5}$ | $X_{i1}$        | $X_{i2}$ | $X_{i3}$ | $X_{i4}$ | $X_{i5}$ | $Y_{i1}$  | $Y_{i2}$ | $Y_{i3}$ | $Y_{i4}$ | $Y_{i5}$ | $Y_{i6}$ |
| 38      | 12                | 40       | 373      | 1600     | 2.15     | 1.00            | 0.00     | 1.00     | 0.60     | 0.13     | 7.10      | 4.4023   | 0.3028   | 253.7183 | 4.2359   | 357      |
| 39      | 12                | 60       | 313      | 800      | 1.83     | 1.00            | 1.00     | -1.00    | -1.00    | -0.21    | 17.21     | 5.9768   | 0.3865   | 227.0327 | 2.1649   | 435.2    |
| 40      | 12                | 60       | 313      | 1400     | 2.04     | 1.00            | 1.00     | -1.00    | 0.20     | 0.02     | 12.10     | 6.3340   | 0.3348   | 243.1633 | 3.2148   | 515      |
| 41      | 12                | 60       | 333      | 800      | 1.68     | 1.00            | 1.00     | -0.33    | -1.00    | -0.37    | 16.40     | 5.8475   | 0.3572   | 234.7569 | 2.6568   | 464.8    |
| 42      | 12                | 60       | 333      | 1000     | 1.74     | 1.00            | 1.00     | -0.33    | -0.60    | -0.30    | 16.22     | 6.1291   | 0.3604   | 235.1529 | 2.9624   | 456.4    |
| 43      | 12                | 60       | 333      | 1200     | 1.78     | 1.00            | 1.00     | -0.33    | -0.20    | -0.26    | 15.50     | 6.0227   | 0.3474   | 239.7327 | 3.0626   | 457.6    |
| 44      | 12                | 60       | 353      | 800      | 1.69     | 1.00            | 1.00     | 0.33     | -1.00    | -0.36    | 15.71     | 5.6397   | 0.3501   | 236.7833 | 2.8259   | 444.4    |
| 45      | 12                | 60       | 353      | 1000     | 1.81     | 1.00            | 1.00     | 0.33     | -0.60    | -0.23    | 15.70     | 5.6300   | 0.3576   | 238.9417 | 3.1271   | 411.8    |
| 46      | 12                | 60       | 353      | 1200     | 1.82     | 1.00            | 1.00     | 0.33     | -0.20    | -0.22    | 13.78     | 5.6666   | 0.3422   | 248.7163 | 3.1848   | 411      |
| 47      | 12                | 60       | 353      | 1400     | 1.95     | 1.00            | 1.00     | 0.33     | 0.20     | -0.08    | 11.25     | 5.9379   | 0.3319   | 258.6363 | 3.4480   | 432.4    |
| 48      | 12                | 60       | 353      | 1400     | 2.08     | 1.00            | 1.00     | 0.33     | 0.20     | 0.06     | 10.80     | 5.4442   | 0.3065   | 265.7493 | 3.3653   | 449.2    |

In the second stage, regression modeling was performed to determine the relation between factors and their corresponding responses which are shown in Table 4. The depiction of the full quadratic regression model is presented by Eq. (5)

$$Y = \beta_0 + \sum_{i=1}^k \beta_i X_i + \sum_{i=1}^k \beta_{ii} X_i^2 + \sum_{i < j}^k \beta_{ij} X_i X_j + \varepsilon \tag{5}$$

where, the response is represented by  $Y$ ,  $\beta$  terms are the model coefficients,  $X$  terms ( $X_i$ : linear terms,  $X_i^2$ : quadratic terms, and  $X_i X_j$ : the interaction of defined parameters) are the factors, and  $\varepsilon$  is residual terms (Atmanli et al., 2015; Ileri et al., 2013; Montgomery, 2017; Yilmaz et al., 2016). Computations for the regression modeling and statistical tests for the significance of the models were performed using the Minitab statistical analysis program. The suggested equation for  $Y$  is given in Eqs. (6) to (11). In these equations,  $\hat{Y}$  represents the estimated regression equations from the observations. The surface plots for the responses are presented in Eqs. (6) to (11) are given in Figures 1 to 6, respectively.

$$\hat{Y}_1 = -103.5669 - 8.4408X_1 - 0.0154X_2 + 0.8624X_3 + 0.0213X_4 - 1.7107X_5 + 0.5600X_1^2 - 0.0049X_2^2 - 0.0010X_3^2 - 0.000003X_4^2 - 0.1544X_5^2 + 0.0941X_1X_2 - 0.0134X_1X_3 - 0.0004X_1X_4 - 0.1252X_1X_5 - 0.0008X_2X_3 - 0.00003X_2X_4 - 0.1417X_2X_5 - 0.00003X_3X_4 + 0.0189X_3X_5 - 0.0021X_4X_5 \tag{6}$$

$$\hat{Y}_2 = -11.0006 + 5.3826X_1 + 0.0685X_2 + 0.0195X_3 - 0.0058X_4 - 9.5937X_5 - 0.2059X_1^2 - 0.0002X_2^2 - 0.00002X_3^2 - 0.0000002X_4^2 + 1.6950X_5^2 + 0.0029X_1X_2 - 0.0037X_1X_3 + 0.0002X_1X_4 - 0.0964X_1X_5 - 0.00006X_2X_3 + 0.00002X_2X_4 - 0.0308X_2X_5 + 0.000006X_3X_4 + 0.0067X_3X_5 + 0.0011X_4X_5 \tag{7}$$

$$\hat{Y}_3 = +2.5723 - 0.1694X_1 - 0.0043X_2 - 0.0080X_3 - 0.0003X_4 + 0.3773X_5 + 0.0045X_1^2 - 0.000004X_2^2 + 0.000006X_3^2 - 0.00000005X_4^2 - 0.0299X_5^2 + 0.0005X_1X_2 + 0.0003X_1X_3 + 0.00001X_1X_4 - 0.0203X_1X_5 - 0.000002X_2X_3 - 0.0000006X_2X_4 + 0.0004X_2X_5 + 0.0000009X_3X_4 - 0.0001X_3X_5 - 0.00002X_4X_5 \tag{8}$$

$$\hat{Y}_4 = -2389.3600 + 246.9574X_1 - 1.8389X_2 + 8.9268X_3 + 0.1334X_4 - 289.8011X_5 - 8.3618X_1^2 + 0.0174X_2^2 - 0.0085X_3^2 + 0.00004X_4^2 + 0.5406X_5^2 - 0.1426X_1X_2 - 0.2709X_1X_3 - 0.0070X_1X_4 + 17.0157X_1X_5 + 0.0033X_2X_3 + 0.0003X_2X_4 + 0.1546X_2X_5 - 0.0003X_3X_4 + 0.2896X_3X_5 - 0.0085X_4X_5 \tag{9}$$

$$\hat{Y}_5 = +44.1671 - 4.8900X_1 + 0.1200X_2 - 0.1333X_3 + 0.0081X_4 - 3.010X_5 + 0.2874X_1^2 + 0.0009X_2^2 + 0.0002X_3^2 - 0.000001X_4^2 + 1.6268X_5^2 - 0.0214X_1X_2 + 0.0025X_1X_3 - 0.0004X_1X_4 - 0.3060X_1X_5 - 0.0001X_2X_3 - 0.000001X_2X_4 + 0.0368X_2X_5 - 0.000006X_3X_4 - 0.01009X_3X_5 + 0.0011X_4X_5 \tag{10}$$

$$\hat{Y}_6 = +4838.9034 - 51.9220X_1 - 63.6828X_2 - 10.9177X_3 - 0.8195X_4 - 492.9323X_5 + 9.0656X_1^2 - 0.0879X_2^2 + 0.0307X_3^2 + 0.00006X_4^2 + 44.4104X_5^2 + 5.0651X_1X_2 - 1.1798X_1X_3 + 0.0610X_1X_4 - 0.7879X_1X_5 + 0.0479X_2X_3 + 0.0031X_2X_4 - 3.0373X_2X_5 - 0.0013X_3X_4 + 0.8753X_3X_5 + 0.1346X_4X_5 \tag{11}$$

The MATLAB programming environment was used for implementing the MSGO. To use these equations in MATLAB for MSGO optimization, models for coded factor levels ranging from -1 to 1 were created. Thus, the models became unit-independent, and multi-objective optimization became straightforward (Ileri et al., 2020; Karaoglan, 2021; Karaoglan and Baydeniz, 2021; Naik et al., 2020). The suggested models based on the coded parameters are presented in Eqs. (12) to (17).

$$\hat{Y}_1 = +8.0519 + 2.6435X_1 - 0.5201X_2 - 0.6861X_3 - 2.2610X_4 - 5.2311X_5 + 1.2601X_1^2 - 1.9734X_2^2 - 0.9384X_3^2 - 0.6777X_4^2 - 0.1350X_5^2 + 2.8243X_1X_2 - 0.6036X_1X_3 - 0.2707X_1X_4 - 0.1757X_1X_5 - 0.4804X_2X_3 - 0.3294X_2X_4 - 2.6500X_2X_5 - 0.4096X_3X_4 + 0.5314X_3X_5 - 0.9971X_4X_5 \tag{12}$$

$$\hat{Y}_2 = +5.5156 - 0.0699X_1 + 0.5846X_2 - 0.4551X_3 + 0.3906X_4 - 1.1433X_5 - 0.4632X_1^2 - 0.0752X_2^2 - 0.0188X_3^2 - 0.0626X_4^2 + 1.4818X_5^2 + 0.0879X_1X_2 - 0.1674X_1X_3 + 0.1435X_1X_4 - 0.1353X_1X_5 - 0.0386X_2X_3 + 0.2256X_2X_4 - 0.5756X_2X_5 + 0.0893X_3X_4 + 0.1889X_3X_5 + 0.5177X_4X_5 \tag{13}$$

$$\hat{Y}_3 = +0.2980 + 0.0147X_1 - 0.0029X_2 - 0.0158X_3 - 0.0412X_4 - 0.0020X_5 + 0.0101X_1^2 - 0.0016X_2^2 + 0.0050X_3^2 - 0.0139X_4^2 - 0.0261X_5^2 + 0.0143X_1X_2 + 0.0117X_1X_3 + 0.0099X_1X_4 - 0.0284X_1X_5 - 0.0011X_2X_3 - 0.0060X_2X_4 + 0.0085X_2X_5 + 0.0139X_3X_4 - 0.0029X_3X_5 - 0.0103X_4X_5 \tag{14}$$

$$\hat{Y}_4 = +274.8283 - 2.9079X_1 - 2.8972X_2 + 13.8230X_3 + 22.2601X_4 - 13.5718X_5 - 18.8142X_1^2 + 6.9547X_2^2 - 7.7374X_3^2 + 10.3432X_4^2 + 0.4726X_5^2 - 4.2793X_1X_2 - 12.1918X_1X_3 - 5.2610X_1X_4 + 23.8646X_1X_5 + 1.9744X_2X_3 + 2.7634X_2X_4 + 2.8903X_2X_5 - 5.0982X_3X_4 + 8.1250X_3X_5 - 3.9938X_4X_5 \tag{15}$$

$$\hat{Y}_5 = +2.7840 + 0.0293X_1 - 0.0007X_2 + 0.2543X_3 + 0.8034X_4 - 0.1117X_5 + 0.6468X_1^2 + 0.3669X_2^2 + 0.1959X_3^2 - 0.2484X_4^2 + 1.4222X_5^2 - 0.6417X_1X_2 + 0.1120X_1X_3 - 0.2916X_1X_4 - 0.4293X_1X_5 - 0.0736X_2X_3 - 0.0105X_2X_4 + 0.6883X_2X_5 - 0.0966X_3X_4 - 0.2832X_3X_5 + 0.5421X_4X_5 \tag{16}$$

$$\hat{Y}_6 = +338.0262 + 21.1987X_1 - 64.4885X_2 - 7.9878X_3 - 36.4228X_4 + 30.3046X_5 + 20.3976X_1^2 - 35.1558X_2^2 + 27.6710X_3^2 + 16.1399X_4^2 + 38.8247X_5^2 + 151.9544X_1X_2 - 53.0932X_1X_3 + 45.7818X_1X_4 - 1.1051X_1X_5 + 28.7274X_2X_3 + 31.0271X_2X_4 - 56.7977X_2X_5 - 20.0685X_3X_4 + 24.5529X_3X_5 + 62.9365X_4X_5 \tag{17}$$

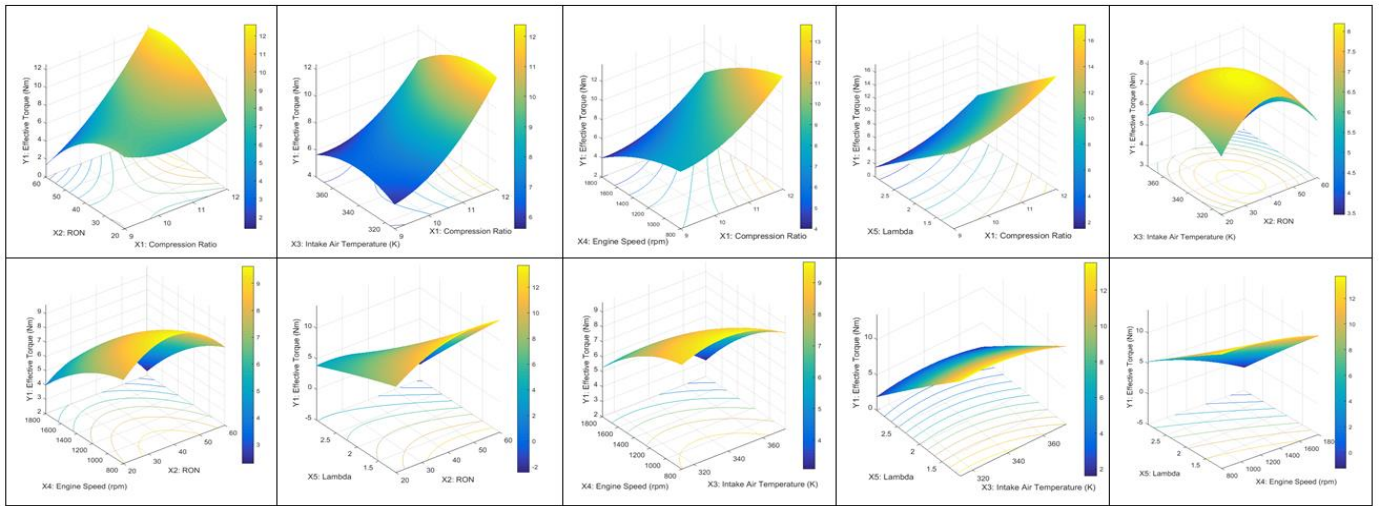


Figure 1. Response surface of Effective Torque (Nm)

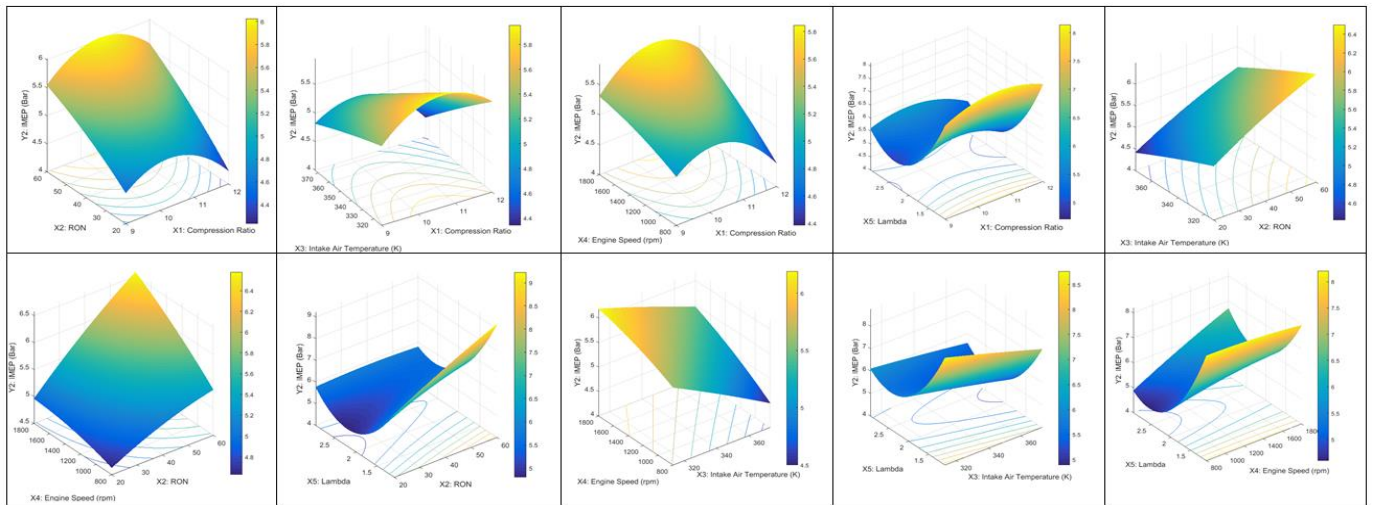


Figure 2. Response surface of IMEP (Bar)

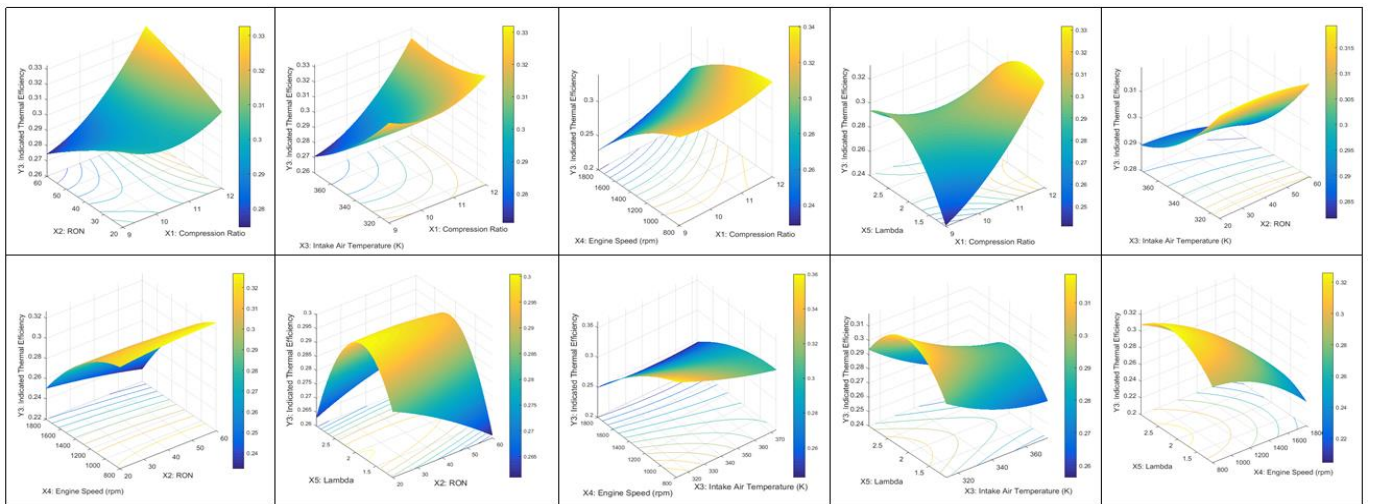


Figure 3. Response surface of Indicated Thermal Efficiency

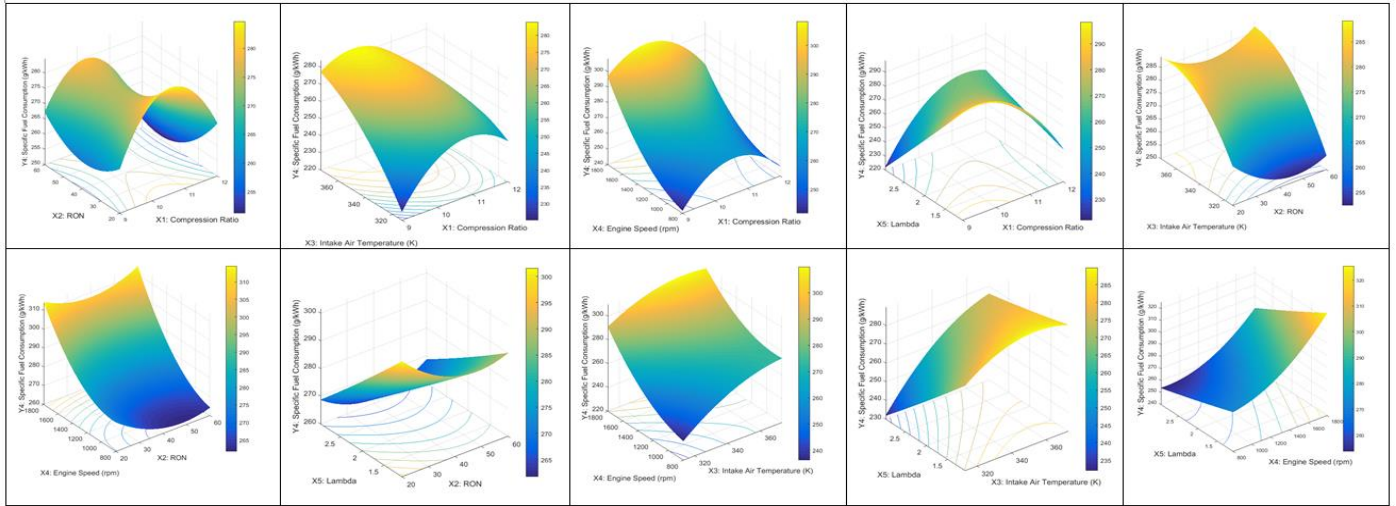


Figure 4. Response surface of Specific Fuel Consumption (g/kWh)

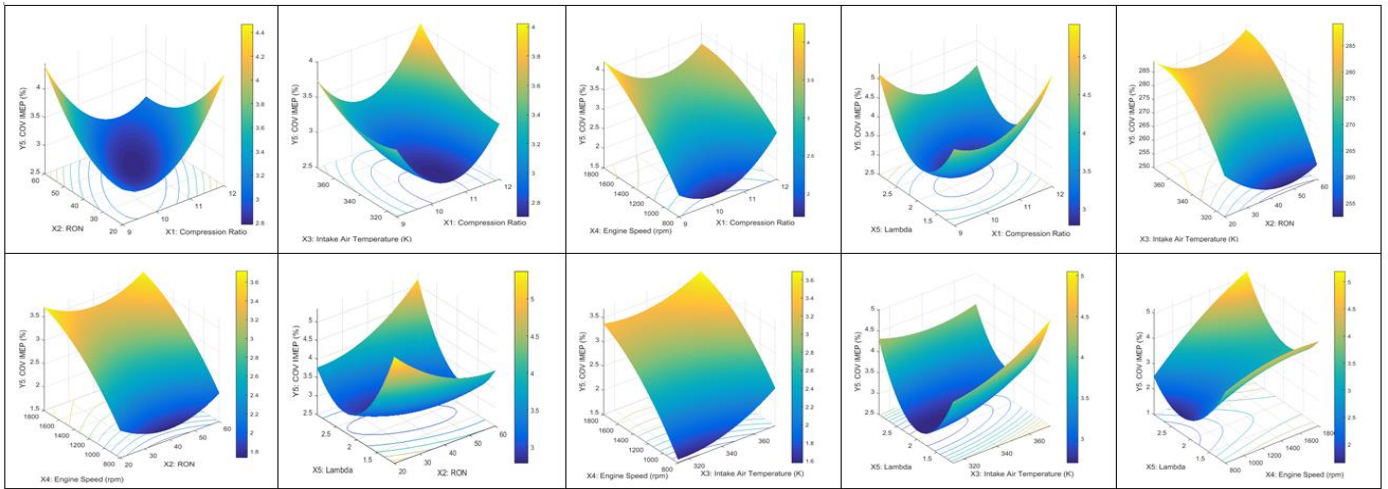


Figure 5. Response surface of COV IMEP (%)

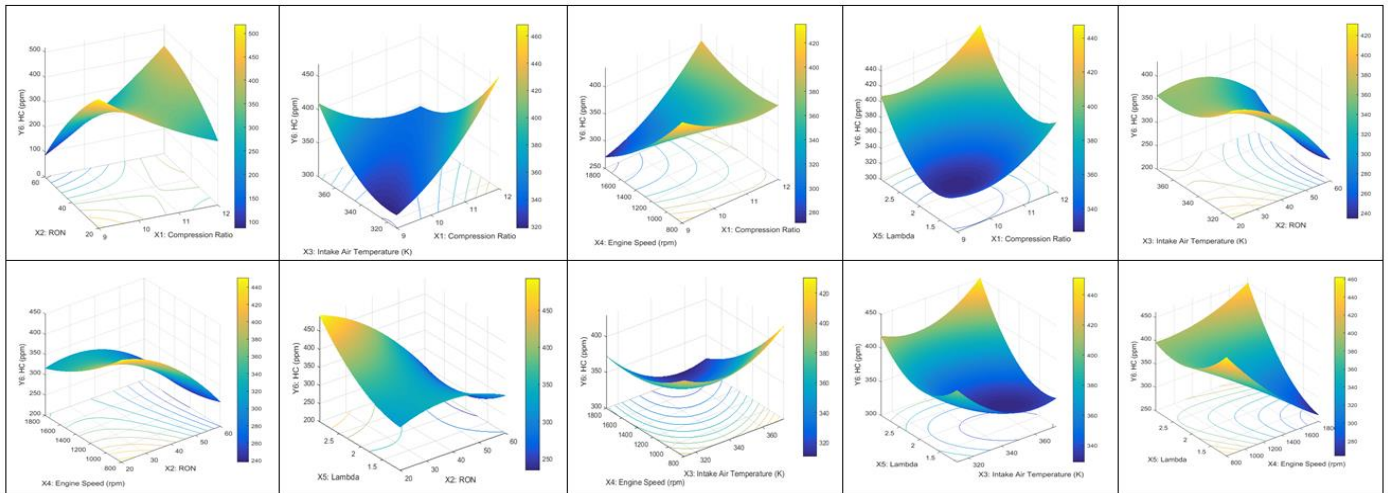


Figure 6. Response surface of HC (ppm)

The  $R^2$  values as an indicator for determining the accuracy of the model are shown in Table 5. The values given in Table 5 indicated that the compression ratio ( $X_1$ ), RON ( $X_2$ ), intake air temperature ( $X_3$ ), engine speed ( $X_4$ ), and lambda ( $X_5$ ) are sufficient to model the responses (effective torque, IMEP, indicated thermal efficiency, specific fuel consumption, COV IMEP, and HC), which means that there is no need to add additional factors to the mathematical models. Then, the mathematical models' significances are tested with the aid of analysis of variance (ANOVA) (Table 6). Table 6 indicates that the models presented in Eqs. (6) to (11), also the same as in Eqs. (12) to (17), are significant. Table 7 shows the prediction performance of the models. Observed responses (measured experimental results from the experimental set-up) are represented by  $Y_i$  in this table, whereas Minitab results (predicted values by the aid of fitted mathematical models) are the  $\hat{Y}_i$  values.  $\hat{Y}_i$  values are rounded to two decimals for a simpler view.  $PE_i$  denotes the prediction error of the  $i$ th run as calculated using Eq. (18).

$$PE_i(\%) = 100(|Y_i - \hat{Y}_i| / \hat{Y}_i) \quad (18)$$

**Table 5.** The  $R^2$  values for the studied responses.

| $R^2$                 | Responses   |             |             |             |             |             |
|-----------------------|-------------|-------------|-------------|-------------|-------------|-------------|
|                       | $\hat{Y}_1$ | $\hat{Y}_2$ | $\hat{Y}_3$ | $\hat{Y}_4$ | $\hat{Y}_5$ | $\hat{Y}_6$ |
| $R^2$ (%)             | 98.41       | 96.68       | 96.74       | 96.84       | 97.26       | 95.97       |
| $R^2$ (prediction)(%) | 91.30       | 84.45       | 91.02       | 81.57       | 76.37       | 76.10       |
| $R^2$ (adjusted) (%)  | 97.24       | 94.22       | 94.32       | 94.50       | 95.23       | 92.99       |

| Studied parameters                | P-value    | significant       |
|-----------------------------------|------------|-------------------|
| Effective torque (Nm)             | 0.000<0.05 | Model Significant |
| IMEP (Bar)                        | 0.000<0.05 | Model Significant |
| Indicated thermal efficiency      | 0.000<0.05 | Model Significant |
| Specific fuel consumption (g/kWh) | 0.000<0.05 | Model Significant |
| COV IMEP (%)                      | 0.000<0.05 | Model Significant |
| HC (ppm)                          | 0.000<0.05 | Model Significant |

**Table 6.** The ANOVA results

**Table 7.** Prediction performance of the models

| Run (i) | Factors  |          |          |          |          |          | Effective torque (Nm) |               |          | IMEP (Bar)     |               |          | Indicated thermal efficiency |               |  |
|---------|----------|----------|----------|----------|----------|----------|-----------------------|---------------|----------|----------------|---------------|----------|------------------------------|---------------|--|
|         | $X_{i1}$ | $X_{i2}$ | $X_{i3}$ | $X_{i4}$ | $X_{i5}$ | $Y_{i1}$ | $\hat{Y}_{i1}$        | $PE_{i1}$ (%) | $Y_{i2}$ | $\hat{Y}_{i2}$ | $PE_{i2}$ (%) | $Y_{i3}$ | $\hat{Y}_{i3}$               | $PE_{i3}$ (%) |  |
| 1       | 9        | 20       | 353      | 1800     | 1.71     | 6.78     | 6.66                  | 1.74          | 4.60     | 4.57           | 0.66          | 0.24     | 0.24                         | 0.51          |  |
| 2       | 9        | 20       | 373      | 800      | 1.6      | 9.45     | 9.26                  | 2.02          | 4.79     | 4.76           | 0.68          | 0.29     | 0.29                         | 1.37          |  |
| 3       | 9        | 20       | 373      | 1200     | 1.68     | 8.42     | 8.49                  | 0.77          | 4.64     | 4.59           | 1.08          | 0.27     | 0.28                         | 3.20          |  |
| 4       | 9        | 20       | 373      | 1200     | 1.99     | 7.86     | 7.95                  | 1.11          | 4.35     | 4.27           | 1.89          | 0.29     | 0.29                         | 0.06          |  |
| 5       | 9        | 40       | 373      | 800      | 1.63     | 8.80     | 8.84                  | 0.40          | 5.02     | 5.25           | 4.25          | 0.27     | 0.28                         | 0.82          |  |
| 6       | 9        | 40       | 373      | 1200     | 1.5      | 8.34     | 8.49                  | 1.72          | 5.69     | 5.73           | 0.78          | 0.26     | 0.26                         | 2.22          |  |
| 7       | 10       | 20       | 313      | 1600     | 1.97     | 5.30     | 4.98                  | 6.51          | 5.10     | 5.22           | 2.29          | 0.29     | 0.29                         | 0.19          |  |
| 8       | 10       | 40       | 313      | 800      | 1.09     | 12.45    | 12.51                 | 0.50          | 9.05     | 8.84           | 2.38          | 0.32     | 0.32                         | 0.60          |  |
| 9       | 10       | 40       | 313      | 800      | 1.38     | 10.92    | 11.12                 | 1.83          | 7.27     | 7.50           | 3.04          | 0.34     | 0.34                         | 0.20          |  |
| 10      | 10       | 40       | 333      | 1200     | 1.81     | 8.75     | 8.93                  | 1.96          | 5.90     | 5.92           | 0.43          | 0.30     | 0.31                         | 0.86          |  |
| 11      | 10       | 40       | 353      | 1000     | 2.31     | 6.92     | 6.83                  | 1.28          | 4.85     | 4.83           | 0.30          | 0.31     | 0.31                         | 1.71          |  |
| 12      | 10       | 40       | 353      | 1200     | 1.92     | 8.05     | 8.02                  | 0.42          | 5.47     | 5.42           | 0.96          | 0.30     | 0.29                         | 2.83          |  |
| 13      | 10       | 40       | 353      | 1600     | 1.68     | 7.17     | 7.46                  | 3.91          | 6.03     | 6.02           | 0.14          | 0.25     | 0.26                         | 0.48          |  |
| 14      | 10       | 60       | 353      | 800      | 1.6      | 8.69     | 8.40                  | 3.42          | 6.85     | 6.43           | 6.45          | 0.29     | 0.29                         | 0.15          |  |
| 15      | 10       | 60       | 353      | 1000     | 1.65     | 7.69     | 7.59                  | 1.28          | 6.34     | 6.45           | 1.60          | 0.28     | 0.29                         | 2.72          |  |
| 16      | 11       | 40       | 353      | 800      | 2.56     | 7.66     | 8.08                  | 5.25          | 4.34     | 4.28           | 1.41          | 0.31     | 0.31                         | 1.70          |  |
| 17      | 11       | 60       | 373      | 800      | 1.58     | 10.72    | 10.65                 | 0.67          | 5.68     | 5.93           | 4.09          | 0.30     | 0.30                         | 0.14          |  |
| 18      | 11       | 60       | 373      | 800      | 1.68     | 10.23    | 9.97                  | 2.56          | 5.53     | 5.57           | 0.75          | 0.31     | 0.31                         | 1.18          |  |
| 19      | 12       | 20       | 313      | 800      | 2.89     | 6.55     | 6.43                  | 1.89          | 4.46     | 4.48           | 0.52          | 0.30     | 0.30                         | 0.15          |  |
| 20      | 12       | 20       | 313      | 1000     | 1.65     | 10.10    | 9.44                  | 7.02          | 5.09     | 5.37           | 5.15          | 0.35     | 0.34                         | 0.78          |  |
| 21      | 12       | 20       | 313      | 1000     | 1.76     | 8.84     | 9.13                  | 3.20          | 5.03     | 5.11           | 1.39          | 0.35     | 0.34                         | 3.12          |  |
| 22      | 12       | 20       | 313      | 1200     | 1.71     | 9.33     | 8.91                  | 4.77          | 5.19     | 5.26           | 1.37          | 0.32     | 0.33                         | 3.90          |  |
| 23      | 12       | 20       | 313      | 1200     | 1.9      | 7.45     | 8.29                  | 10.14         | 4.92     | 4.91           | 0.07          | 0.34     | 0.33                         | 2.37          |  |
| 24      | 12       | 20       | 313      | 1200     | 2.18     | 6.85     | 7.36                  | 6.99          | 4.89     | 4.63           | 5.53          | 0.31     | 0.32                         | 2.41          |  |
| 25      | 12       | 20       | 313      | 1400     | 1.82     | 7.20     | 7.92                  | 9.10          | 5.17     | 5.09           | 1.68          | 0.32     | 0.32                         | 0.52          |  |
| 26      | 12       | 20       | 313      | 1400     | 2.18     | 7.05     | 6.58                  | 7.12          | 4.71     | 4.75           | 0.92          | 0.30     | 0.30                         | 0.67          |  |
| 27      | 12       | 20       | 313      | 1600     | 1.94     | 6.65     | 6.58                  | 1.04          | 5.07     | 4.97           | 1.99          | 0.30     | 0.29                         | 1.27          |  |
| 28      | 12       | 20       | 373      | 800      | 2.96     | 6.65     | 6.50                  | 2.29          | 3.59     | 3.62           | 0.86          | 0.25     | 0.25                         | 0.13          |  |
| 29      | 12       | 40       | 313      | 800      | 1.67     | 15.45    | 15.61                 | 1.01          | 6.50     | 6.05           | 7.54          | 0.37     | 0.37                         | 0.76          |  |
| 30      | 12       | 40       | 313      | 1000     | 1.71     | 14.59    | 15.12                 | 3.50          | 6.27     | 6.06           | 3.46          | 0.34     | 0.36                         | 4.60          |  |
| 31      | 12       | 40       | 313      | 1200     | 1.77     | 15.26    | 14.26                 | 7.02          | 5.97     | 6.03           | 0.97          | 0.35     | 0.35                         | 0.40          |  |
| 32      | 12       | 40       | 333      | 800      | 1.69     | 15.80    | 15.62                 | 1.12          | 5.29     | 5.48           | 3.43          | 0.35     | 0.35                         | 1.33          |  |
| 33      | 12       | 40       | 333      | 1000     | 1.76     | 15.70    | 14.88                 | 5.54          | 5.22     | 5.45           | 4.24          | 0.35     | 0.35                         | 1.40          |  |
| 34      | 12       | 40       | 353      | 800      | 1.71     | 15.34    | 14.82                 | 3.49          | 4.91     | 4.90           | 0.21          | 0.34     | 0.34                         | 0.37          |  |
| 35      | 12       | 40       | 353      | 1200     | 2.43     | 9.57     | 9.72                  | 1.58          | 4.25     | 4.36           | 2.63          | 0.31     | 0.31                         | 1.56          |  |
| 36      | 12       | 40       | 373      | 800      | 1.74     | 12.58    | 13.16                 | 4.41          | 4.46     | 4.28           | 4.22          | 0.33     | 0.33                         | 1.23          |  |
| 37      | 12       | 40       | 373      | 1200     | 1.94     | 10.72    | 10.71                 | 0.07          | 4.46     | 4.33           | 2.84          | 0.33     | 0.33                         | 0.28          |  |
| 38      | 12       | 40       | 373      | 1600     | 2.15     | 7.10     | 6.98                  | 1.65          | 4.40     | 4.61           | 4.61          | 0.30     | 0.30                         | 0.06          |  |
| 39      | 12       | 60       | 313      | 800      | 1.83     | 17.21    | 16.47                 | 4.50          | 5.98     | 6.09           | 1.82          | 0.39     | 0.38                         | 1.47          |  |
| 40      | 12       | 60       | 313      | 1400     | 2.04     | 12.10    | 12.46                 | 2.89          | 6.33     | 6.32           | 0.18          | 0.33     | 0.33                         | 0.94          |  |
| 41      | 12       | 60       | 333      | 800      | 1.68     | 16.40    | 17.47                 | 6.13          | 5.85     | 6.11           | 4.23          | 0.36     | 0.36                         | 1.72          |  |
| 42      | 12       | 60       | 333      | 1000     | 1.74     | 16.22    | 16.48                 | 1.56          | 6.13     | 6.15           | 0.41          | 0.36     | 0.36                         | 0.88          |  |
| 43      | 12       | 60       | 333      | 1200     | 1.78     | 15.50    | 15.39                 | 0.74          | 6.02     | 6.28           | 4.11          | 0.35     | 0.35                         | 0.41          |  |
| 44      | 12       | 60       | 353      | 800      | 1.69     | 15.71    | 16.36                 | 3.98          | 5.64     | 5.52           | 2.12          | 0.35     | 0.35                         | 0.42          |  |
| 45      | 12       | 60       | 353      | 1000     | 1.81     | 15.70    | 14.81                 | 5.98          | 5.63     | 5.42           | 3.82          | 0.36     | 0.35                         | 2.57          |  |
| 46      | 12       | 60       | 353      | 1200     | 1.82     | 13.78    | 13.84                 | 0.45          | 5.67     | 5.68           | 0.30          | 0.34     | 0.34                         | 0.40          |  |
| 47      | 12       | 60       | 353      | 1400     | 1.95     | 11.25    | 11.61                 | 3.12          | 5.94     | 5.66           | 4.96          | 0.33     | 0.33                         | 1.72          |  |
| 48      | 12       | 60       | 353      | 1400     | 2.08     | 10.80    | 10.49                 | 2.96          | 5.44     | 5.42           | 0.47          | 0.31     | 0.32                         | 5.07          |  |

**Table 7.** Continued.

| Run (i) | Specific fuel consumption (g/kWh) |                |               |          | COV IMEP (%)   |               |          |                | HC (ppm)      |  |  |  |
|---------|-----------------------------------|----------------|---------------|----------|----------------|---------------|----------|----------------|---------------|--|--|--|
|         | $Y_{i4}$                          | $\hat{Y}_{i4}$ | $PE_{i4}$ (%) | $Y_{i5}$ | $\hat{Y}_{i5}$ | $PE_{i5}$ (%) | $Y_{i6}$ | $\hat{Y}_{i6}$ | $PE_{i6}$ (%) |  |  |  |
| 1       | 322.72                            | 319.12         | 1.13          | 4.26     | 4.18           | 1.86          | 392      | 374.0          | 4.81          |  |  |  |
| 2       | 283.52                            | 284.40         | 0.31          | 3.22     | 3.12           | 3.16          | 687.8    | 697.4          | 1.37          |  |  |  |
| 3       | 288.26                            | 288.93         | 0.23          | 3.78     | 3.80           | 0.55          | 585.8    | 558.2          | 4.95          |  |  |  |
| 4       | 282.06                            | 278.46         | 1.30          | 3.27     | 3.36           | 2.68          | 567.6    | 586.2          | 3.17          |  |  |  |
| 5       | 275.13                            | 275.90         | 0.28          | 2.78     | 2.96           | 6.16          | 543      | 538.3          | 0.88          |  |  |  |
| 6       | 284.62                            | 289.29         | 1.61          | 4.19     | 4.02           | 4.23          | 397      | 419.0          | 5.25          |  |  |  |
| 7       | 271.95                            | 280.07         | 2.90          | 3.49     | 3.43           | 1.94          | 405      | 422.3          | 4.10          |  |  |  |
| 8       | 255.75                            | 255.44         | 0.12          | 3.30     | 3.23           | 2.06          | 488      | 494.6          | 1.33          |  |  |  |
| 9       | 251.95                            | 247.24         | 1.90          | 2.23     | 2.41           | 7.62          | 461      | 456.6          | 0.96          |  |  |  |
| 10      | 269.05                            | 267.57         | 0.55          | 2.72     | 2.67           | 1.72          | 360.8    | 342.5          | 5.35          |  |  |  |
| 11      | 266.08                            | 264.18         | 0.72          | 2.35     | 2.34           | 0.36          | 389      | 384.3          | 1.22          |  |  |  |

| Run (i) | Specific fuel consumption (g/kWh) |                |               | COV IMEP (%) |                |               | HC (ppm) |                |               |
|---------|-----------------------------------|----------------|---------------|--------------|----------------|---------------|----------|----------------|---------------|
|         | $Y_{i4}$                          | $\hat{Y}_{i4}$ | $PE_{i4}(\%)$ | $Y_{i5}$     | $\hat{Y}_{i5}$ | $PE_{i5}(\%)$ | $Y_{i6}$ | $\hat{Y}_{i6}$ | $PE_{i6}(\%)$ |
| 12      | 273.95                            | 276.79         | 1.03          | 2.65         | 2.79           | 5.04          | 366.2    | 349.4          | 4.81          |
| 13      | 305.76                            | 303.81         | 0.64          | 3.26         | 3.47           | 5.91          | 263.6    | 287.3          | 8.26          |
| 14      | 271.96                            | 275.74         | 1.37          | 2.85         | 2.65           | 7.85          | 296.8    | 287.1          | 3.38          |
| 15      | 282.92                            | 279.13         | 1.36          | 2.98         | 3.00           | 0.81          | 242.8    | 249.6          | 2.73          |
| 16      | 266.42                            | 266.47         | 0.02          | 2.22         | 2.02           | 9.78          | 373      | 384.4          | 2.96          |
| 17      | 269.89                            | 266.20         | 1.38          | 3.12         | 3.09           | 0.81          | 400      | 395.3          | 1.20          |
| 18      | 264.15                            | 267.17         | 1.13          | 2.86         | 2.92           | 2.16          | 392      | 384.8          | 1.88          |
| 19      | 253.75                            | 254.28         | 0.21          | 3.12         | 3.20           | 2.56          | 429.4    | 424.1          | 1.26          |
| 20      | 249.14                            | 251.37         | 0.89          | 4.49         | 4.50           | 0.35          | 372.4    | 378.0          | 1.48          |
| 21      | 245.42                            | 251.53         | 2.43          | 4.33         | 4.24           | 2.11          | 342      | 377.7          | 9.44          |
| 22      | 259.42                            | 256.42         | 1.17          | 4.46         | 4.61           | 3.26          | 378.6    | 363.4          | 4.18          |
| 23      | 255.51                            | 256.39         | 0.34          | 4.24         | 4.26           | 0.48          | 381.4    | 369.6          | 3.19          |
| 24      | 260.25                            | 256.42         | 1.50          | 4.09         | 3.96           | 3.50          | 393.6    | 384.6          | 2.34          |
| 25      | 264.51                            | 264.48         | 0.01          | 4.51         | 4.59           | 1.76          | 373.6    | 360.4          | 3.65          |
| 26      | 269.91                            | 263.88         | 2.28          | 4.32         | 4.24           | 1.79          | 376.6    | 388.1          | 2.97          |
| 27      | 275.51                            | 275.45         | 0.02          | 4.49         | 4.58           | 1.95          | 365      | 370.6          | 1.52          |
| 28      | 279.64                            | 280.36         | 0.26          | 3.80         | 3.80           | 0.10          | 343      | 339.2          | 1.13          |
| 29      | 227.82                            | 229.71         | 0.83          | 3.07         | 2.94           | 4.26          | 518.4    | 482.8          | 7.37          |
| 30      | 236.62                            | 232.72         | 1.68          | 3.14         | 3.19           | 1.71          | 496      | 472.1          | 5.06          |
| 31      | 242.60                            | 238.96         | 1.53          | 3.55         | 3.36           | 5.45          | 446.6    | 468.2          | 4.61          |
| 32      | 236.82                            | 239.26         | 1.02          | 3.15         | 3.10           | 1.41          | 421.6    | 423.2          | 0.37          |
| 33      | 237.65                            | 241.42         | 1.56          | 3.31         | 3.28           | 0.88          | 408.2    | 407.1          | 0.27          |
| 34      | 241.82                            | 242.16         | 0.14          | 3.39         | 3.43           | 1.16          | 359.8    | 388.8          | 7.46          |
| 35      | 255.46                            | 256.21         | 0.29          | 3.23         | 3.44           | 6.04          | 372      | 380.5          | 2.23          |
| 36      | 247.12                            | 238.66         | 3.55          | 3.85         | 3.91           | 1.54          | 395      | 379.5          | 4.09          |
| 37      | 240.78                            | 243.29         | 1.03          | 4.14         | 4.03           | 2.73          | 346.4    | 345.6          | 0.24          |
| 38      | 253.72                            | 260.01         | 2.42          | 4.24         | 4.14           | 2.30          | 357      | 358.5          | 0.43          |
| 39      | 227.03                            | 225.16         | 0.83          | 2.16         | 2.33           | 6.95          | 435.2    | 473.3          | 8.06          |
| 40      | 243.16                            | 247.00         | 1.55          | 3.21         | 3.21           | 0.26          | 515      | 504.1          | 2.17          |
| 41      | 234.76                            | 234.43         | 0.14          | 2.66         | 2.63           | 0.97          | 464.8    | 456.6          | 1.80          |
| 42      | 235.15                            | 237.79         | 1.11          | 2.96         | 2.86           | 3.70          | 456.4    | 449.4          | 1.56          |
| 43      | 239.73                            | 244.02         | 1.76          | 3.06         | 3.05           | 0.25          | 457.6    | 452.4          | 1.16          |
| 44      | 236.78                            | 238.44         | 0.70          | 2.83         | 2.94           | 4.02          | 444.4    | 441.2          | 0.74          |
| 45      | 238.94                            | 241.93         | 1.24          | 3.13         | 3.07           | 1.83          | 411.8    | 425.0          | 3.11          |
| 46      | 248.72                            | 246.39         | 0.94          | 3.18         | 3.28           | 2.92          | 411      | 427.0          | 3.75          |
| 47      | 258.64                            | 256.05         | 1.01          | 3.45         | 3.38           | 1.89          | 432.4    | 432.4          | 0.00          |
| 48      | 265.75                            | 258.14         | 2.95          | 3.37         | 3.40           | 1.08          | 449.2    | 431.3          | 4.14          |

**Table 8.** The results of verifications

| Run (i) | Factors  |          |          |          | Effective torque (Nm) |          |                |               | IMEP (Bar) |                |               | Indicated thermal efficiency |                |               |
|---------|----------|----------|----------|----------|-----------------------|----------|----------------|---------------|------------|----------------|---------------|------------------------------|----------------|---------------|
|         | $X_{i1}$ | $X_{i2}$ | $X_{i3}$ | $X_{i4}$ | $X_{i5}$              | $Y_{i1}$ | $\hat{Y}_{i1}$ | $PE_{i1}(\%)$ | $Y_{i2}$   | $\hat{Y}_{i2}$ | $PE_{i2}(\%)$ | $Y_{i3}$                     | $\hat{Y}_{i3}$ | $PE_{i3}(\%)$ |
| 49      | 9        | 20       | 333      | 1000     | 1.45                  | 9.59     | 9.64           | 0.54          | 5.98       | 5.67           | 5.49          | 0.31                         | 0.32           | 2.40          |
| 50      | 9        | 20       | 353      | 1600     | 1.75                  | 6.90     | 7.57           | 8.79          | 5.05       | 4.62           | 9.42          | 0.25                         | 0.27           | 4.93          |
| 51      | 9        | 40       | 373      | 1400     | 1.63                  | 7.58     | 7.11           | 6.58          | 5.84       | 5.45           | 7.19          | 0.25                         | 0.25           | 1.56          |
| 52      | 9        | 40       | 373      | 1400     | 1.72                  | 7.24     | 6.67           | 8.60          | 5.48       | 5.27           | 3.99          | 0.24                         | 0.25           | 4.57          |
| 53      | 10       | 40       | 333      | 1400     | 1.67                  | 8.56     | 9.02           | 5.12          | 6.40       | 6.29           | 1.70          | 0.28                         | 0.28           | 0.84          |
| 54      | 10       | 40       | 353      | 1000     | 1.95                  | 7.97     | 8.54           | 6.64          | 5.57       | 5.22           | 6.62          | 0.32                         | 0.31           | 4.61          |
| 55      | 10       | 40       | 353      | 1400     | 1.72                  | 7.42     | 8.24           | 9.91          | 6.00       | 5.89           | 1.92          | 0.27                         | 0.28           | 1.37          |
| 56      | 10       | 60       | 333      | 800      | 1.35                  | 10.10    | 10.76          | 6.17          | 7.83       | 7.91           | 1.05          | 0.32                         | 0.30           | 7.66          |
| 57      | 12       | 40       | 353      | 800      | 1.81                  | 14.68    | 14.38          | 2.10          | 4.57       | 4.62           | 1.07          | 0.37                         | 0.34           | 8.88          |
| 58      | 12       | 40       | 353      | 800      | 1.99                  | 13.24    | 13.57          | 2.43          | 4.43       | 4.21           | 5.16          | 0.36                         | 0.34           | 7.58          |
| 59      | 12       | 40       | 373      | 1200     | 1.94                  | 10.72    | 10.71          | 0.07          | 4.46       | 4.33           | 2.84          | 0.33                         | 0.33           | 0.28          |
| 60      | 12       | 40       | 373      | 1200     | 2.22                  | 9.79     | 9.31           | 5.18          | 4.24       | 4.03           | 5.31          | 0.32                         | 0.32           | 1.23          |
| 61      | 12       | 60       | 333      | 1200     | 1.89                  | 14.71    | 14.45          | 1.82          | 5.93       | 5.97           | 0.74          | 0.35                         | 0.34           | 2.67          |

**Table 8.** Continued.

| Run (i) | Specific fuel consumption (g/kWh) |                |               | COV IMEP (%) |                |               | HC (ppm) |                |               |
|---------|-----------------------------------|----------------|---------------|--------------|----------------|---------------|----------|----------------|---------------|
|         | $Y_{i4}$                          | $\hat{Y}_{i4}$ | $PE_{i4}(\%)$ | $Y_{i5}$     | $\hat{Y}_{i5}$ | $PE_{i5}(\%)$ | $Y_{i6}$ | $\hat{Y}_{i6}$ | $PE_{i6}(\%)$ |
| 49      | 263.53                            | 268.64         | 1.90          | 3.08         | 3.21           | 4.28          | 593      | 574.6          | 3.21          |
| 50      | 319.86                            | 301.02         | 6.26          | 4.07         | 3.94           | 3.29          | 431      | 424.8          | 1.46          |
| 51      | 293.40                            | 294.90         | 0.51          | 4.23         | 4.12           | 2.53          | 335      | 368.2          | 9.01          |
| 52      | 305.63                            | 291.97         | 4.68          | 4.39         | 4.03           | 8.72          | 381.4    | 372.0          | 2.54          |
| 53      | 283.49                            | 282.01         | 0.52          | 3.30         | 3.09           | 6.72          | 287      | 317.0          | 9.46          |
| 54      | 265.40                            | 270.46         | 1.87          | 2.22         | 2.37           | 6.37          | 342.6    | 380.5          | 9.97          |
| 55      | 291.74                            | 290.14         | 0.55          | 3.23         | 3.24           | 0.37          | 300.4    | 315.9          | 4.89          |
| 56      | 260.82                            | 266.35         | 2.08          | 3.05         | 2.77           | 9.91          | 309.8    | 293.7          | 5.47          |
| 57      | 230.55                            | 243.95         | 5.49          | 3.21         | 3.22           | 0.29          | 384.2    | 383.7          | 0.12          |
| 58      | 235.61                            | 247.20         | 4.69          | 2.98         | 2.92           | 1.87          | 357      | 376.8          | 5.26          |
| 59      | 240.78                            | 243.29         | 1.03          | 4.14         | 4.03           | 2.73          | 346.4    | 345.6          | 0.24          |
| 60      | 251.95                            | 249.06         | 1.16          | 3.82         | 3.80           | 0.52          | 361.6    | 359.3          | 0.65          |
| 61      | 236.86                            | 245.33         | 3.45          | 3.06         | 3.00           | 1.81          | 485.2    | 444.8          | 9.08          |

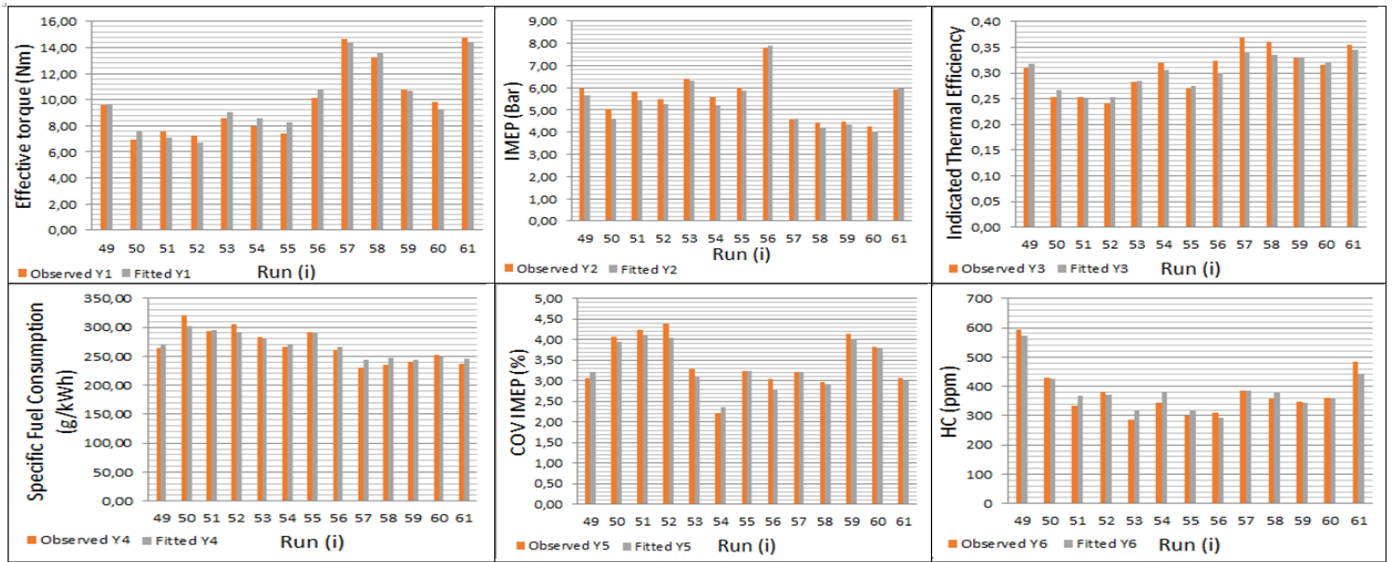


Figure 7. The verification results of the suggested models

Table 8 depicts the verification results of the suggested models. In the verification phase, 13 additional experimental runs that were not used in the mathematical modeling phase were performed (Figure 7).

The presented results in Tables 7 and 8 show that the suggested models could successfully fit the experimental data with a high accuracy. The MSGO algorithm was performed using MATLAB. The maximum number of iterations and population size were chosen as 30 and 2000, respectively. The number of search agents and the number of iterations were determined by the suggested values in the literature (Naik, 2021; Naik et al., 2020). The studied issue assumed as a constrained continuous optimization problem in the modeling process (Ileri et al., 2020; Karaoglan, 2021; Karaoglan and Baydeniz, 2021). The regression models presented in Eqs. (12) to (17) were applied for this purpose. The importance of the responses at the optimization phase is defined by giving weights to them in the goal function Z. The weights for [Y1-Y6] are defined as 20%, 5%, 10%, 20%, 20%, and 25% respectively.

$$Z = +(0.20)|\hat{Y}_{1,coded} / \max(Y_{i1})| + (0.05)|\hat{Y}_{2,coded} / \max(Y_{i2})| + (0.10)|\hat{Y}_{3,coded} / \max(Y_{i3})| - (0.20)|\hat{Y}_{4,coded} / \max(Y_{i4})| - (0.20)|\hat{Y}_{5,coded} / \max(Y_{i5})| - (0.25)|\hat{Y}_{6,coded} / \max(Y_{i6})| \quad (19)$$

$$\min Z \text{ s.t. } X_1 \in [-1,1]; X_2 \in [-1,1]; X_3 \in [-1,1]; X_4 \in [-1,1]; X_5 \in [-1,1] \quad (20)$$

The max ( $Y_i$ ) values are shown in Table 4. Table 9 shows the verification results for this optimized factor-level combination. The results indicate that the overall PE (%) is acceptable. The PE (%) for HC (ppm) seems quite high but if you notice, the experimentally observed value for the HC (ppm) value that is desired to be minimized is much lower than the estimated value.

## References

- Abdelmalek, Z., Alamian, R., Safdari Shadloo, M., Maleki, A., & Karimipour, A. (2021). Numerical study on the performance of a homogeneous charge compression ignition engine fueled with different blends of biodiesel. *Journal of Thermal Analysis and Calorimetry*, 143(3), 2695-2705. <https://doi.org/10.1007/s10973-020-09513-1>
- AlShabi, M., Ghenai, C., Bettayeb, M., Ahmad, F. F., & El Haj Assad, M. (2021). Multi-group grey wolf optimizer (MG-GWO) for estimating photovoltaic solar cell model. *Journal of Thermal Analysis and Calorimetry*, 144(5), 1655-1670. <https://doi.org/10.1007/s10973-020-09895-2>
- Atmanli, A., Yüksel, B., Ileri, E., & Karaoglan, A. D. (2015). Response surface methodology based optimization of diesel-n-butanol-cotton oil ternary blend ratios to improve engine performance and exhaust emission

Therefore, although the PE (%) value is 13.08%, the observed value is actually lower than expected in a positive way.

Table 9. Verification for the suggested values

| Optimized responses               | Observed ( $Y_i$ ) | Predicted ( $\hat{Y}_i$ ) | PE <sub>i</sub> (%) |
|-----------------------------------|--------------------|---------------------------|---------------------|
| Effective torque (Nm)             | 16.58              | 17.92                     | 7.48                |
| IMEP (Bar)                        | 6.63               | 6.73                      | 1.49                |
| Indicated thermal efficiency      | 0.36               | 0.38                      | 5.26                |
| Specific fuel consumption (g/kWh) | 228.36             | 224.16                    | 1.87                |
| COV IMEP (%)                      | 2.54               | 2.52                      | 0.79                |
| HC (ppm)                          | 432.4              | 497.49                    | 13.08               |

## 4. Conclusions

This study aimed to examine the recently invented and promising human-based optimization algorithm known as modified social group optimization to optimize LTC HCCI engine performance, combustion, and emission parameters. The following conclusions are drawn from this study:

- The calculated  $R^2$  obtained from this study show that the compression ratio ( $X_1$ ), RON ( $X_2$ ), intake air temperature ( $X_3$ ), engine speed ( $X_4$ ), and lambda ( $X_5$ ) are sufficient to model the responses (effective torque, IMEP, indicated thermal efficiency, specific fuel consumption, COV IMEP, and HC).
- In the verification phase of this study, 13 additional experimental runs that were not used in the mathematical modeling phase were used. It was found that the regression models fit the observed values well with a low PE (%).
- The MSGO algorithm suggested the best value for studied parameters as  $X_1=11.47$ ,  $X_2=60$ ,  $X_3=313$ ,  $X_4=800$ , and  $X_5=1.45$ . The Verification results show satisfying results with a high performance.
- The results indicate that the recently invented MSGO algorithm can effectively optimize these types of problems.

- characteristics. *Energy Conversion and Management*, 90, 383-394. <https://doi.org/10.1016/j.enconman.2014.11.029>
- Bhadoria, A., & Marwaha, S. (2020). Moth flame optimizer-based solution approach for unit commitment and generation scheduling problem of electric power system. *Journal of Computational Design and Engineering*, 7(5), 668-683. <https://doi.org/10.1093/jcde/qwaa050>
- Calam, A., Solmaz, H., Yilmaz, E., & İçingür, Y. (2019). Investigation of effect of compression ratio on combustion and exhaust emissions in a HCCI engine. *Energy*, 168, 1208-1216. <https://doi.org/10.1016/j.energy.2018.12.023>
- Deh Kiani, M. K., Ghobadian, B., Tavakoli, T., Nikbakht, A. M., & Najafi, G. (2010). Application of artificial neural networks for the prediction of performance

- and exhaust emissions in SI engine using ethanol- gasoline blends. *Energy*, 35(1), 65-69.  
<https://doi.org/10.1016/j.energy.2009.08.034>
- Eiben, A. E., & Schippers, C. A. (1998). On evolutionary exploration and exploitation. *Fundamenta Informaticae*, 35(1-4), 35-50.  
<https://doi.org/10.3233/FI-1998-35123403>
- Heidari, A. A., Mirjalili, S., Faris, H., Aljarah, I., Mafarja, M., & Chen, H. (2019). Harris hawks optimization: Algorithm and applications. *Future generation computer systems*, 97, 849-872.  
<https://doi.org/10.1016/j.future.2019.02.028>
- Ileri, E., Karaoglan, A. D., & Akpinar, S. (2020). Optimizing cetane improver concentration in biodiesel-diesel blend via grey wolf optimizer algorithm. *Fuel*, 273, 117784. <https://doi.org/10.1016/j.fuel.2020.117784>
- Ileri, E., Karaoglan, A. D., & Atmanli, A. (2013). Response surface methodology based prediction of engine performance and exhaust emissions of a diesel engine fuelled with canola oil methyl ester. *Journal of Renewable and Sustainable Energy*, 5(3), 033132. <https://doi.org/10.1063/1.4811801>
- Karaoglan, A. D. (2021). Optimizing Plastic Extrusion Process via Grey Wolf Optimizer Algorithm and Regression Analysis. *Journal of Scientific and Industrial Research*, 80(01), 34-41.
- Karaoglan, A. D., & Baydeniz, B. (2021). Optimizing Plastic Injection Process Using Whale Optimization Algorithm in Automotive Lighting Parts Manufacturing. *Journal of Scientific and Industrial Research*, 80(04), 360-368.
- Kocakulak, T., Babagiray, M., Nacak, Ç., Safieddin Ardebili, S. M., Calam, A., & Solmaz, H. (2022). Multi objective optimization of HCCI combustion fuelled with fusel oil and n-heptane blends. *Renewable Energy*, 182, 827-841.  
<https://doi.org/https://doi.org/10.1016/j.renene.2021.10.041>
- Kocakulak, T., Halis, S., Ardebili, S. M. S., Babagiray, M., Haşimoğlu, C., Rabeti, M., & Calam, A. (2023). Predictive modelling and optimization of performance and emissions of an auto-ignited heavy naphtha/n-heptane fueled HCCI engine using RSM. *Fuel*, 333, 126519.  
<https://doi.org/https://doi.org/10.1016/j.fuel.2022.126519>
- Leo, G. M. L., Sekar, S., & Arivazhagan, S. (2020). Experimental investigation and ANN modelling of the effects of diesel/gasoline premixing in a waste cooking oil-fuelled HCCI-DI engine. *Journal of Thermal Analysis and Calorimetry*, 141(6), 2311-2324. <https://doi.org/10.1007/s10973-020-09418-z>
- Mirjalili, S. (2016). SCA: a sine cosine algorithm for solving optimization problems. *Knowledge-based systems*, 96, 120-133.  
<https://doi.org/10.1016/j.knsys.2015.12.022>
- Mirjalili, S., & Lewis, A. (2016). The whale optimization algorithm. *Advances in engineering software*, 95, 51-67.  
<https://doi.org/10.1016/j.advengsoft.2016.01.008>
- Mirjalili, S., Mirjalili, S. M., & Lewis, A. (2014). Grey wolf optimizer. *Advances in engineering software*, 69, 46-61.  
<https://doi.org/10.1016/j.advengsoft.2013.12.007>
- Moghdani, R., & Salimifard, K. (2018). Volleyball premier league algorithm. *Applied Soft Computing*, 64, 161-185.  
<https://doi.org/10.1016/j.asoc.2017.11.043>
- Montgomery, D. C. (2017). *Design and analysis of experiments*. John Wiley & sons.
- Naik, A. (2021). *Modified Social Group Optimization Algorithm*. MATLAB Central File Exchange. Retrieved 21 September from <https://www.mathworks.com/matlabcentral/fileexchange/78272-modified-social-group-optimization-algorithm>
- Naik, A., Satapathy, S. C., & Abraham, A. (2020). Modified Social Group Optimization—a meta-heuristic algorithm to solve short-term hydrothermal scheduling. *Applied Soft Computing*, 95, 106524. <https://doi.org/10.1016/j.asoc.2020.106524>
- Nematollahi, A. F., Rahiminejad, A., & Vahidi, B. (2017). A novel physical based meta-heuristic optimization method known as Lightning Attachment Procedure Optimization. *Applied Soft Computing*, 59, 596-621. <https://doi.org/10.1016/j.asoc.2017.06.033>
- Nematollahi, A. F., Rahiminejad, A., & Vahidi, B. (2020). A novel meta-heuristic optimization method based on golden ratio in nature. *Soft Computing*, 24(2), 1117-1151. <https://doi.org/10.1007/s00500-019-03949-w>
- Parsa, S., & Neshat, E. (2022). Thermodynamic and statistical analysis on the effect of exhaust gas recirculation on waste heat recovery from homogeneous charge compression ignition engines. *Journal of Thermal Analysis and Calorimetry*, 147(11), 6349-6361.  
<https://doi.org/10.1007/s10973-021-10923-y>
- Rao, R. V., & Keesari, H. S. (2020). A self-adaptive population Rao algorithm for optimization of selected bio-energy systems. *Journal of Computational Design and Engineering*, 8(1), 69-96.  
<https://doi.org/10.1093/jcde/qwaa063>
- Roushangar, K., & Shahrazi, S. (2019). Bed load prediction in gravel-bed rivers using wavelet kernel extreme learning machine and meta-heuristic methods. *International Journal of Environmental Science and Technology*, 16(12), 8197-8208. <https://doi.org/10.1007/s13762-019-02287-6>
- Satapathy, S., & Naik, A. (2016). Social group optimization (SGO): a new population evolutionary optimization technique. *Complex & Intelligent Systems*, 2(3), 173-203. <https://doi.org/10.1007/s40747-016-0022-8>
- Shareef, H., Ibrahim, A. A., & Mutlag, A. H. (2015). Lightning search algorithm. *Applied Soft Computing*, 36, 315-333.  
<https://doi.org/10.1016/j.asoc.2015.07.028>
- Tejani, G. G., Savsani, V. J., Patel, V. K., & Mirjalili, S. (2018). An improved heat transfer search algorithm for unconstrained optimization problems. *Journal of Computational Design and Engineering*, 6(1), 13-32. <https://doi.org/10.1016/j.jcde.2018.04.003>
- Yazdani, M., & Jolai, F. (2015). Lion Optimization Algorithm (LOA): A nature-inspired metaheuristic algorithm. *Journal of Computational Design and Engineering*, 3(1), 24-36. <https://doi.org/10.1016/j.jcde.2015.06.003>
- Yilmaz, N., Ileri, E., Atmanli, A., Deniz Karaoglan, A., Okkan, U., & Sureyya Kocak, M. (2016). Predicting the engine performance and exhaust emissions of a diesel engine fueled with hazelnut oil methyl ester: the performance comparison of response surface methodology and LSSVM. *Journal of Energy Resources Technology*, 138(5), 052206.  
<https://doi.org/10.1115/1.4032941>
- Zhao, W., Wang, L., & Zhang, Z. (2019). A novel atom search optimization for dispersion coefficient estimation in groundwater. *Future Generation Computer Systems*, 91, 601-610.  
<https://doi.org/10.1016/j.future.2018.05.037>